Iranian Journal of Materials Forming11 (2) (2024) 46-61

Online ISSN: 2383-0042

IJMF

Iranian Journal of Materials Forming

Journal Homepage: http://ijmf.shirazu.ac.ir

Research Article

Investigating the Effect of Process Order and Die Shape on the Mechanical Properties of Copper in Combined Severe Plastic Deformation of Twist Extrusion and ECAP

S.A. Zamani[1*], M. Bakhshi-Jooybari[2], H. Gorji[2], S.J. Hosseinipour[3] and M. Hoseinzadeh-Amirdehi[1]

[1] Department of Mechanical Engineering, Faculty of Engineering, Islamic Azad University, Ayatollah Amoli Branch, Amol, Iran
[2] Department of Mechanical Engineering, Faculty of Engineering, Noshirvani University of Technology, Babol, Iran
[3] Department of Materials and Industrial Engineering, Faculty of Engineering, Noshirvani University of Technology, Babol, Iran

ARTICLE INFO

Article history:

Received 5 June 2024
Reviewed 24 June 2024
Accepted 21 August 2024
Revised 24 August 2024

Keywords:

Severe plastic deformation
FEA
Mechanical properties

Please cite this article as:

Zamani, S.A., Bakhshi-Jooybari, M., Gorji, H., Hosseinipour, S.J., & Hoseinzadeh-Amirdehi, M. (2024). Investigating the effect of process order and die shape on the mechanical properties of copper in combined severe plastic deformation of twist extrusion and ECAP. *Iranian Journal of Materials Forming*, *11*(2), 46-61. https://doi.org/10.22099/IJMF.2024.50382.1298

ABSTRACT

Investigating production techniques and enhancing the mechanical properties of fine-grained materials has been a focus of extensive research in recent years. The production of fine-grained materials free from impurities and porosity through severe plastic deformation methods has made these techniques increasingly appealing. In this research, the combined extrusion process was carried out using a die that included two twisting and ECAP channels in two modes: direct and reverse. The forming force, strain, and hardness generated in the specimen were determined using finite element analysis, 2D/3D DEFORM software, and the Vickers micro-hardness test. It was found that the maximum value of the forming force in the reverse process has increased by 30%, while the standard deviation of the strain and hardness values measured in the cross-section of the specimen decreased by 73% and 56%, respectively. This created much more uniform strains in one process passes, which is one of the main goals of the severe plastic deformation method. Evaluating the effect of design variable sizes showed that the average forming force and the maximum strain increased by 48% and 44%, respectively, as the ratio of the large diameter to the small diameter, m, of the elliptical region in the twisting channel of the die increased. Additionally, as the twist angle θ increased, these parameters rose by 35% and 63%, respectively, while an increase in the internal angle of ECAP, α, led to a 33% reduction in the average forming force and a 22% decrease in the maximum strain generated.

1. Introduction

The physical and mechanical properties of crystalline materials are significantly influenced by various parameters, among which the average grain size is particularly important. The control of grain size has long been recognized as a critical factor for designing materials with desirable properties. A metal material is classified as ultrafine if its grain size falls within the range of 100 to 1000 nm, while if the grain size is smaller than 100 nm, the material is referred to as a nanostructure. Over the past two decades, the production of ultrafine metallic materials has garnered considerable attention from researchers [1]

Crystalline metallic materials can be classified into two categories: single crystal and polycrystal. The strength of polycrystalline materials is associated with grain size, as described by the Hall-Petch relation [2]:

* Corresponding author
E-mail address: ali93zamani@gmail.com (S.A. Zamani)
https://doi.org/10.22099/IJMF.2024.50382.1298

$$\tau = \tau_0 + kd^{-1/2} \quad (1)$$

Where $\boldsymbol{\tau_0}$ is the network friction stress and indicates the material's resistance to sliding, k is the grain boundary locking factor, d is the size of the grain diameter in nanometers, and τ is the yield strength of the material in GPa. According to the Hall-Petch relation, the strength of a material increases as the grain size decreases. Reducing the size of the grains or the constituent phases of a material to the nanometer scale or to very fine dimensions, results in significant changes in the material's properties.

In the past decade, researchers have shown considerable interest in the production of ultrafine-grained and nanostructured metallic materials, positioning these materials as a new generation of metal products characterized by optimal ductility. Roven [3] has identified the main areas of industrial applications for these materials, including the manufacture of medical equipment such as high-strength prostheses and implants, as well as applications in the aerospace industry, defense equipment, sports, energy, and the electronics and telecommunications industries, etc.

Extensive research has been conducted at both laboratory and industrial scales to develop nanostructured materials. One of the most effective methods identified for this purpose is severe plastic deformation, a technique first introduced by Bridgman et al. By employing these methods and subjecting specimens to severe strains in one or more stages, researchers can significantly reduce grain size while enhancing mechanical properties without causing noticeable alterations to the overall dimensions of the specimens. Consequently, metal products can be effectively produced in the form of wires or sheets using severe plastic deformation methods. The materials produced via SPD are characterized by their lack of porosity and contamination, making them highly attractive to researchers [4].

In recent years, various severe plastic deformation processes have been introduced, including pressing in the channels of equal channel angular pressing (ECAP) [5], high pressure torsion [6], accumulative roll bonding [7], twist extrusion [8], and friction stir processing [9]. Additionally, a novel method known as elliptic cross-section equal channel extrusion (ECSEE) has been developed, which utilizes a spiral channel with an elliptic cross-section [10].

ECAP is one of the most widely used severe plastic deformation processes. Research findings indicate that this process significantly improves the mechanical properties of the specimen at ambient temperature, in addition to their superplastic ductility at elevated temperatures [11].

In addition to optimizing the geometric dimensions of the die, common strategies to maximize the strain created and enhance the mechanical properties of the material during ECAP include repeating the pressing steps and employing a multi-step die. However, these approaches also have inherent limitations [12, 13].

In their investigation of the kinematics associated with the twist extrusion process, Latypov et al. [14] highlighted a notable similarity to the ECAP method: both processes exhibit a pure shear deformation mode. However, a key distinction lies in the structural configuration of the processes; twist extrusion (TE) incorporates two shear layers one oriented vertically and the other aligned parallel to the axis of the specimen in contrast to the single shear plane characteristic of ECAP. Additionally, the twist extrusion process is characterized by the presence of a semi-eddy flow, which occurs concurrently with the stretching and amalgamation of metal particles. The researchers claimed these unique features of the TE process provide new avenues for the development of refined microstructures. This method has been effective in producing microstructures from a variety of metals such as aluminum, copper, and titanium alloys.

Jiang et al. [15] introduced a novel technique called equal channel reciprocating extrusion (ECRE) to induce severe plastic deformation in 7005 aluminum alloy. The microstructure and mechanical properties of 7005 aluminum alloy subjected to a processing pass were investigated. The results indicated that the severe plastic deformation induced during this process led to the formation of a mixed microstructure, significantly enhancing the ultimate tensile strength of the specimen. The mechanical properties in the fully processed areas of the material were found to be superior to those in the incompletely processed regions, which was attributed

to the effects of dislocation strengthening. It was observed that yield strength and ultimate strength initially decreased and then increased by rising the extrusion temperature. After six passes of the process, the yield and ultimate strength increased to 359.2 and 490 MPa, respectively.

Gupta et al. [16] conducted a study examining the influence of die design parameters on specimens processed through ECAP. In their research, the effect of the following four parameters including, channel angle, corner angle, number of passes, and route type were investigated. The results of the various parameters were compared, revealing that the optimal channel angle for achieving maximum shear strain was 90 degrees. It was observed that as the channel angle increased beyond this value, the shear strain decreased. Additionally, a corner angle of approximately 20 degrees was identified as optimal for effectively filling the die corners. Through 4 to 6 passes of the process using the $\boldsymbol{B_C}$ route, a microstructure characterized by very fine grain refinement was achieved. Subsequently, Al-TiO_2 specimens were processed, and their microstructural and mechanical properties were compared.

In a separate study, Muralidaran et al. [17] proposed a novel integrated severe plastic deformation technique called multi-angular twist extrusion (MATE). Through experimental studies, the researchers optimized several variables of the MATE process, enabling the production of very fine-grained metals with highly uniform strain in a single pass. They investigated the effects of input parameters, including annealing temperature, lubricant type, and extrusion speed, on the size and uniformity of hardness as well as the final tensile strength of the extruded specimens. The optimal parameters for achieving the desired material properties were subsequently determined. Experiments were conducted based on full factorial design and the TOPSIS approach was used to find the optimal combination of input parameters. Variance analysis was used to determine the contribution of input parameters on mechanical properties of the extruded specimens. After finite element analysis, the process was performed with an annealing temperature of

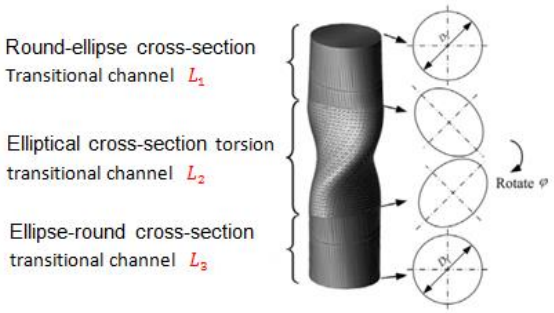

Fig. 1. A schematic illustration of the extrusion process in spiral channels with an elliptical cross-section [22].

550 °C, molybdenum disulfide lubricant, and extrusion speed of 3 mm/s as optimal parameters, and an average effective strain of 2.72 was created in the specimen. Experimental studies showed that the strength and hardness of copper alloy increased by 69.8% and 80.5%, respectively.

In another study, Attarilar et al. [18] investigated the twist extrusion process to determine the optimal parameter values for producing specimens with higher strain and lower forming forces. Their findings revealed that the torsion angle has the most significant influence on the strain behavior of the deformed specimen, accounting for approximately 56% of the effect. Furthermore, the size of the friction coefficient significantly affects the forming force, contributing approximately 31% to its variation, while the geometric dimensions of the specimen influence the strain behavior by about 12%. The specimens used in the study were prepared from pure copper, and the results indicated that, due to microstructural changes, the yield strength and ultimate tensile strength increased by 2.3 and 1.5 times, respectively, compared to the annealed prototype. The hardness of the specimen increased significantly from 46.1 Vickers to 96.7 Vickers. However, the plastic deformation area of the specimen is limited due to the reduction in strain capacity, hardness, and ductility. Additionally, the plastic strain generated in the peripheral region of the specimen's cross-sectional area is higher than that in the central surface, resulting from the higher hardness in the peripheral areas. The deformed copper specimen exhibited a combined microstructure consisting of low angle dislocation walls and high angle grain boundaries.

In another study, Zamani et al. [19] investigated the effect of die parameters on the mechanical properties of pure copper in the combined process of twist extrusion and ECAP and with the help of experimental design using the surface response method and according to the size of the forming force. The results indicated values of 90.5°, 39°, 34 mm, 1.65, and 120° for the created strain, strength, and hardness of the specimens. These values correspond to the optimal parameters related to the geometric dimensions of the die, which include the internal and external angles of the ECAP channel, the length of the twisting area, the ratio of the large diameter to the small diameter of the elliptical area, and the twisting angle of the twisting section, respectively.

Kocisko et al. [20] investigated the influence of the ECAP die channel angle on the deformation behavior of the specimen and the distribution of effective strain across its cross section. To enhance efficiency, they focused on the geometric design of the die and aimed to achieve maximum uniformity in deformation by performing simulations using the DEEORM software. The channel angle, outer radius, and inner radius of the die corner were considered as the main parameters, and the average values of effective plastic strain were calculated for various sizes of these parameters. The simulation results demonstrated that increasing the outer corner angle resulted in a reduction of the average effective strain. Furthermore, by assessing the coefficient of strain non-uniformity in the transverse direction of the specimen, it was determined that after two processing passes, the strain distribution across the cross-sectional surface of the specimens became more uniform.

Bisadi et al. [21], in a study, attempted to combine the ECAP process with the twist extrusion process in order to optimize the ECAP process. Similar to the twisting extrusion process, they considered the inlet and outlet directions of the ECAP channels relative to each other with a twist angle. In order to study the strain distribution in both transverse and longitudinal directions of the specimens, they performed Vickers micro-hardness test and observed that after one pass of the process, the hardness of the specimens in the combined method increases significantly compared to the ECAP. Hardness distribution also becomes more homogeneous in this method.

Elliptic cross-section equal-channel extrusion is another method invented by Wang et al. [22]. This novel technique integrates twist cutting, extrusion, and offset processes, effectively overcoming the limitations of the traditional twist extrusion method, which is confined to extruding specimens with only rectangular cross-sections. Since industrial raw materials typically have a circular cross-section, the twist extrusion process design may be limited to certain industrial applications. However, this method can readily be implemented using standard extrusion equipment to alter the shape of the cumulative twist in order to modify the material properties.

Fig. 1 illustrates the general principles of the described process. In the first section of the die channel, with a length of L_1, the circular cross-section of the specimen is transformed into an oval shape. In the second section, with a length of L_2, the specimen undergoes twisting. Finally, in the third section, with a length of L_3, the elliptical cross-section reverts to a circular shape. During the twisting deformation in the second section, the elliptical cross-section created in the first section gradually rotates under the twisting angle φ to the beginning of the third section. The special shape of the die channel facilitates severe plastic deformation without changing the specimen's cross-sectional area. This feature allows the specimen to be extruded repeatedly, enabling the accumulation of deformation, modification of the microstructure, and improvement of the specimen's properties.

In another study Wang et al. [23] optimized the dimensions of the extrusion die for Elliptic cross-section equal-channel extrusion. This process was conducted by considering the lengths of the extrusion channels (L_1, L_2, L_3), the twist angle φ, and the ratio of the large diameter to the small diameter in the elliptical region of the channel, m, as the design parameters. The optimization indicators, on the other hand, were the average effective strain ε_{ave} and the deformation uniformity coefficient, α, which is defined as $\varepsilon_{ave} / (\varepsilon_{max}-\varepsilon_{min})$. The optimal geometric dimensions of the die were determined using the Grey theory.

In another study, Heydari et al. [24] investigated the effect of die geometry on the grain size distribution and plasticity properties using simulation in DEFORM software in the TCAP process. For this,

they used dies with internal angles of 90°, 100° and 110°, external angles of 0°, 10° and 20° and twist angles of 30°, 45° and 60°. In addition, the location of the twist channel was examined before and after the ECAP location. The distribution of plastic strain, grain size distribution, and the required punch force for the TCAP process on aluminum alloy 7050 were extracted in all conditions. The results showed that locating the twist section after ECAP location led to a better microstructure in the billet. Moreover, the die with a twist angle of 45°, an internal angle of 110°, and a corner angle of 0° created the best results and the grain size decreased from 100 µm to 3.67 µm.

In all methods of severe plastic deformation, the primary objectives are to create maximum uniform strain in the specimens, resulting in a finer grain structure and, consequently, higher strength and hardness. To achieve this, it is necessary to repeat each process over several steps, allowing the strain to increase incrementally until the desired value is reached. However, this approach can be challenging and time-consuming. Additionally, the hardness values are often non-uniform across the cross-section of the specimens, depending on the strain values.

In order to simultaneously use the capabilities of the two processes of twisting extrusion and ECAP, in this research, a combined die that includes twisting and ECAP channels was prepared and the process was carried out in two modes configurations. In the first case, the copper specimen entered the twisting channel and then exited from the ECAP channel, which was called direct extrusion in this research. In the second case, the specimen first entered the ECAP channel and then exited through the twisting channel, which is called reverse extrusion. In each case, simulations were used to compare the forming force requirements and the strain generated in the specimen. The effect of the size of the design variables on the forming force and the resulting strain was then investigated. To investigate uniformity of the created structure, a hardness test was done experimentally for both cases and the results were compared. This study has assisted in achieving one of the main goals of severe plastic deformation processes, which is a more uniform increase of strain values in the cross-sectional area of the specimen and creating a homogeneous structure in a smaller number of passes, has been achieved in only one pass of the combined process.

2. Experimental Procedure

Fig. 2 represents a specimen used in the experiments. The specimens were made of pure copper, and were selected from extruded rods with a diameter of 16 mm and subsequently machined to achieve a diameter of approximately 15 mm and a length of 60 mm. To improve the softness, cold working ability, and plasticity of the specimens, they were first annealed, and then the oxide layer on their surface was removed with sandpaper.

Fig. 3 shows the schematic of the die, where D represents the diameter of the channel, L is the length of the twisting area, α is the ECAP angle, and ψ is the corner angle in the ECAP region. In order to provide a better representation of the twist position, the image of this area of the die was also shown.

Table 1 illustrates the geometrical specifications of the die, where **θ** represents the twist angle of the twisting area, and m denotes the ratio of the large diameter to the small diameter of the elliptical section in the twisting channel of the die.

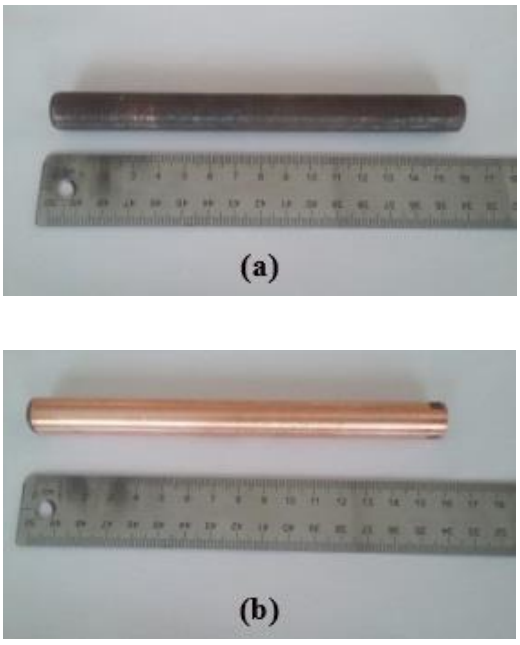

Fig. 2. Images of the annealed specimen: (a) before deoxidation and (b) after deoxidation.

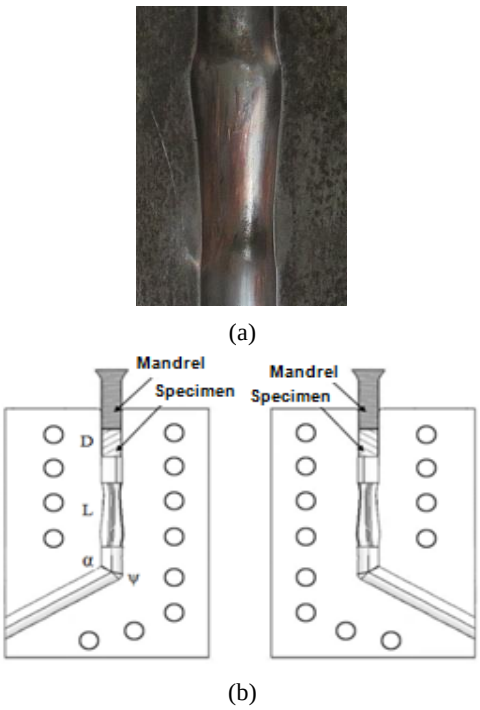

(a)

(b)

Fig. 3. (a) Image of die twist area and (b) schematic of the combined die with mandrel and specimen.

Table 1. Geometrical specifications of the die

Parameter	value
L (mm)	52
m	1.55
θ (degree)	120
α (degree)	120
ψ (degree)	37

Spark emission spectroscopy quantometer was used to assess the chemical characteristics of the specimens. The chemical composition of the specimens is presented in Table 2, while their mechanical and physical properties are shown in Table 3.

Table 2. Chemical composition of copper specimen (weight percentage)

Mg	Ni	Pb	Zn	Sn	Mn	Cu
0.003	0.030	0.010	0.011	0.002	0.009	**Base**

Table 3. Mechanical and physical characteristics of the pure copper specimen [25]

Poisson's ratio	Young modulus (GPa)	Ultimate tensile strength (MPa)	Yield strength (MPa)	Density (kg/m^3)
0.343	270	270	180	8930

Fig. 4 shows true stress-true strain curve of annealed pure copper and tensile specimen. In addition, the Hollomon equation was used to describe the plastic deformation behavior of the specimen:

$$\sigma = K\varepsilon^{n} \quad (2)$$

Where σ, ε, K, and n are effective von Mises stress, effective plastic strain, strength coefficient, and strain hardening exponent, respectively. The magnitude of the strength coefficient K and strain hardening exponent n obtained by tensile test according to ASTM-E8 as 518 and 0.46 MPa, respectively.

Among the conventional paths for conducting the ECAP process, path B_c is recognized as the most effective for producing ultrafine materials. Therefore, this path was employed for forming the specimens in both dies in this study. Hence, during the repetition steps, the specimens were rotated 90 degrees in a fixed direction around their central axis.

The hardness of the specimens was measured using the Vickers hardness test with the HVS-1000A micro-hardness device, in accordance with the ASTM E-384 standard. During the test, a compressive force of 0.2 kg was applied, followed by a pause time of 10 seconds.

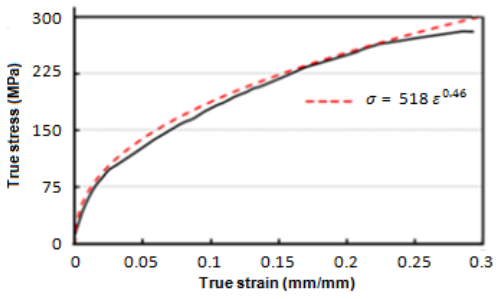

(a)

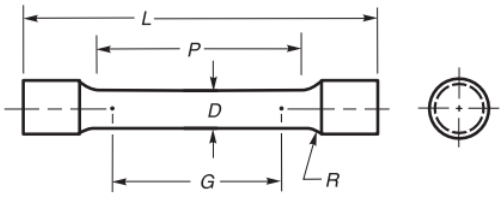

L	P	R	D	G
90	75	9	12.5	62.5

(b)

Fig. 4. (a) True stress-true strain curve of pure annealed copper specimen and (b) specimen dimensions [26].

To determine the variations in hardness at different points across the cross-section of the specimens, transverse cuts were made near the exit points of each specimen from the dies. After cold mounting, the specimens were completely polished by sanding and polishing, and subsequently prepared for hardness measurement.

Hardness values were measured at six distinct points along the radial distances from the center to the periphery of each specimen. To evaluate the hardness distribution across the cross-section of the specimens, the standard deviation was calculated for each case, and the results were subsequently compared.

To apply the required force for the process, a Denison Mayes Group (DMG) universal press with a capacity of 600 kN, available at the Research Center of Modern Material Forming Processes at Noshirvani University of Technology in Babol, was utilized. Both processes were carried out at a uniform pressing speed of 2 mm/s. To minimize friction between the specimen and the die, the specimen was wrapped in teflon tape, and the die channels were lubricated with common industrial oil.

For the experimental test of this research, a die was employed in two separate configurations, as depicted in Fig. 5. The first configuration was designed for direct extrusion, while the second configuration was intended for reverse extrusion. Since the specimen is pressed vertically, a support with an inclination matching the slope of the ECAP channel was applied to facilitate the reverse extrusion process. All experimental tests were performed under the same conditions and at ambient temperature.

As shown in Fig. 5, the die features two separate channels of the same diameter, including a spiral channel with an elliptical cross-section and an ECAP channel. Constructed from MO40 material, the die consists of two completely symmetrical halves that were subjected to heat treatment after machining. Firstly, in order to relieve the created stress after machining, the die was preheated in the initial furnace at a temperature of about 600 °C for 3.5 hours. Then, it was placed in a furnace at 860 °C for about one hour, and then it was quenched by turbulent oil at about

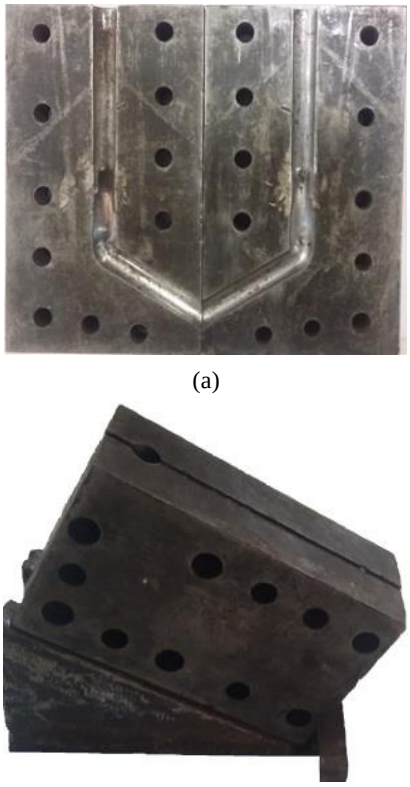

(a)

(b)

Fig. 5. (a) The direct extrusion die and (b) the reverse extrusion die with a support.

50 °C. After that, in order to perform precipitation hardening, the die was placed in a furnace at 200 °C for one hour and then tempered at 330 °C, which eventually reached a hardness of about 55HRC. The internal surfaces of the die were polished to ensure cleanliness, and guide pins were used to align the two halves. They were secured together with several screws.

Due to the high forming force, using a long mandrel may result in bending. 200VCN bar was utilized for their construction and they were fabricated in several shorter segments as shown in Fig. 6, which were then employed sequentially.

Fig. 6. The manufactured punch, divided into smaller parts.

It should be noted that the mandrels do not enter the spiral area of the die; instead, they only move to the beginning of this area and push the copper specimen forward. However, since it is necessary to completely remove the specimen from the die, after the mandrels reach the beginning of the spiral region, the following steps are taken:

- The die is inverted, and small blows are applied to remove the mandrels.
- A short copper rod is placed between the specimen and the mandrels, acting as a sacrificial.
- Pressure is again applied by the mandrels.

This process continues until the specimen is completely removed from the die.

3. Experiment Design Using the Response Surface Methodology (RSM)

The design variables for the three dies investigated in this study are detailed in Table 4.

Table 4. Variable values at three different levels

Parameter	level 1	level 2	level 3
m	1.45	1.55	1.65
θ (degree)	60	90	120
α (degree)	90	105	120

Typically, to conduct an experimental test or simulation for a research study involving k variables, each with n levels, the total number of tests required is equal to n^k, resulting in an exponential increase. Given this issue, the current research, which includes three-level variables, requires conducting 27 distinct simulations, a task that proves to be quite complex. Therefore, in order to reduce the number of simulations and make the research more manageable, an experimental design has been used. The main goal of the experimental design is to appropriately discretize the design space and select the most relevant and effective simulation models for process investigation.

For this purpose, the test matrix was designed using the Design Expert software, taking into account the number of studied variables, expected accuracy, and other relevant factors. This matrix includes seven different modes, as shown in Table 5. It should be noted that, to verify the accuracy of the results, the software suggests some modes multiple times.

Table 5. Experiment design matrix

Die (mode)	Run	m	θ (degree)	α (degree)
1	1	1.55	120	120
2	2	1.55	90	105
3	3	1.55	90	120
4	4	1.55	60	120
1	5	1.55	120	120
5	6	1.65	90	90
3	7	1.55	90	120
5	8	1.65	90	90
6	9	1.45	90	90
7	10	1.55	90	90

4. Simulation of Finite Elements

Using DEFORM-2D/3D V: 11.0 software, the finite element method was employed to calculate the required forming force, strain generated in the specimen and its distribution during the modeling of the combined process. The model of the combined die is made up of three components: a deformable rod or specimen, a die, and a cylindrical mandrel, both of which are considered rigid. In this setup, the die is secured in all directions, and the advance is applied to the mandrel.

The Hollomon equation, $\sigma=k\varepsilon^n$, was used to describe the plastic deformation behavior of the specimen, where k represents the strength coefficient and n indicates the strain hardening exponent. From the true stress-strain curve obtained during the experimental tensile test, the values of k and n were determined to be 518 MPa and 0.46, respectively.

To determine the appropriate friction coefficient and validate the simulation results, the load-displacement diagram obtained from the experimental twist extrusion process was compared with the diagram generated from the simulated model using three different friction coefficients. Fig. 7 illustrates that the simulation with a friction coefficient of 0.1 closely matched the experimental results, showing a maximum difference of only 5%. This strong correlation led to the selection of the Coulomb friction model, which employs a uniform friction coefficient of 0.1 for all surfaces, as the appropriate option for the simulations. During the simulation, the friction between the specimen, dies and mandrels was considered uniform at all points.

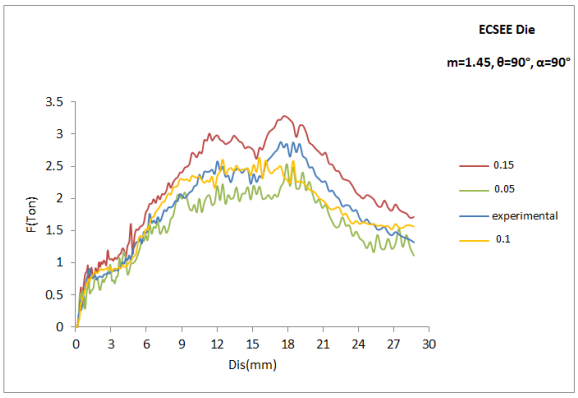

Fig. 7. Load-displacement diagram in experimental and simulation mode with different friction coefficients.

The simulated model of the combined die, shown in Fig. 8, includes a meshed specimen composed of two separate channels with equal diameters, a twisting channel and an ECAP channel.

The elliptical spiral geometry of the die necessitated a fully three-dimensional modeling approach for both the part and the die, with the specimen assumed to be isotropic. Considering that the number of grid elements can affect the accuracy of finite element analysis output, a comparison was made between several grid choices. Convergence analysis was used to determine the size and number of elements needed in the simulations. According to Fig. 9, it can be seen that the number of elements is more than 32000. Due to the selection of the tetrahedral element with the smallest dimension of about 0.5 mm, the number of elements was automatically selected about 32004. To facilitate convergence during the process simulation, which involved high strains and deformations, an automatic meshing method was employed.

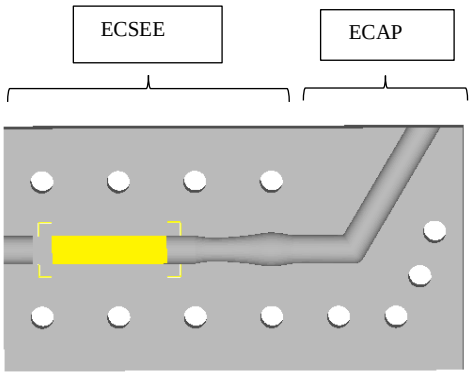

Fig. 8. Finite element model created by DEFORM software.

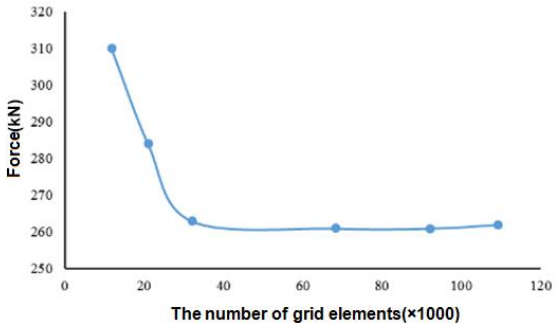

Fig. 9. Element size sensitivity diagram.

5. Results and Discussion

5.1. Effect of process order

5.1.1. Forming force

The load-displacement diagram of the direct extrusion process, as depicted in Fig. 10, demonstrates that as the specimen is first extruded through the twisting channel and the L_1 area of the die channel, its circular cross-section gradually transforms into an elliptical shape and the force curve exhibits a gentle increasing trend. As the specimen enters the twist deformation area L_2 of the die channel, the additional twist shear stress contributes to an increase in the forming force, resulting in a significant rise in force. In the final stage, when the specimen enters the L_3 area of the die channel, the force curve begins to show a decreasing trend as the cross-section transforms from an elliptical shape back to a circular shape. The force decreases as the specimen fully exits the twisting channel and before the ECAP process begins, which is attributed to the short distance between the two areas. Upon entering the ECAP area, the forming force experiences a noticeable increase. Subsequently, after the specimen has completely passed through this area, the force curve begins to show a decreasing trend.

The load-displacement diagram of the reverse extrusion process is presented in Fig. 11. Upon entering the twisting area, the forming force experiences a jump, and the force curve remains at its peak until the specimen exits this area. Following passage through the twisting area, the curve begins to show a decreasing trend. Before the specimen completely exits the twisting region, the ECAP region begins, resulting in an increase in the force curve once more. Finally, after leaving the ECAP region, the force value decreases.

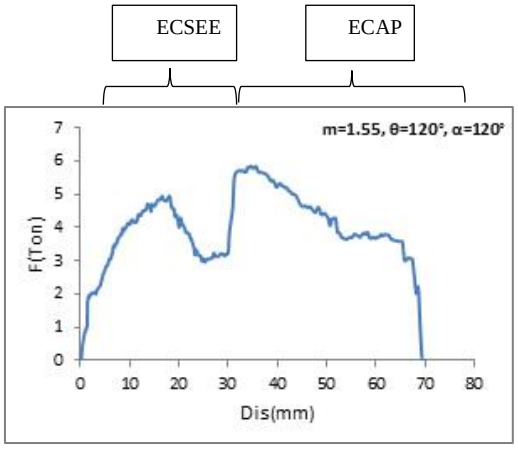

Fig. 10. Load-displacement diagram of direct extrusion process.

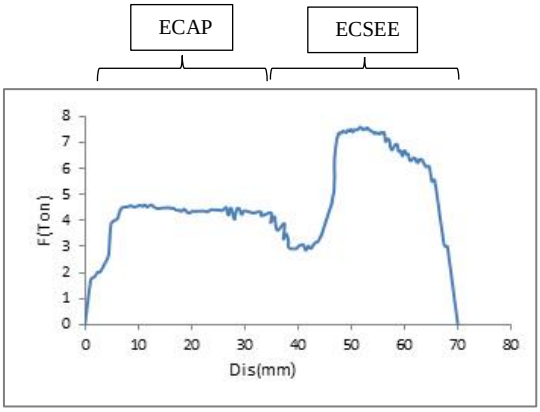

Fig. 11. Load-displacement diagram of reverse extrusion process.

Comparing Fig. 12 and 13 reveals that the maximum forming force in the reverse extrusion process increased by approximately 30%, from 5.85 tons to 7.6 tons. The dimensional change of the grain size after the ECAP process is the primary factor contributing to this increase. The grains near the die wall experience tension due to the friction between the specimen and the wall, resulting in greater strain and larger dimensions compared to other parts of the specimen's cross-sectional surface. The twist extrusion process, being a type of severe plastic deformation that yields a very homogeneous structure, logically results in a significant increase in the forming force at the beginning. As the specimen moves through the twisting area of the die, the forming force gradually decreases. Ultimately, after the specimen exits this area, the force approaches zero.

5.1.2. Strain

The strain distribution diagrams and strain histograms for specimens from both direct and reverse extrusion processes are illustrated in Fig. 12. In combined processes of severe plastic deformation, the total final strain in the specimen is cumulative, thus, altering the order of the processes does not significantly impact the magnitude of the final strain. In the reverse extrusion process, the average final strain is 1.08, which is only 0.01 lower than that of the direct process, a difference that is not considered statistically significant. Fig. 13 illustrates the strain distribution curves with the histogram diagrams in the cross-section of the specimens at the exit point of the dies. Similar to the previous case, the average size of the strain produced in the two processes is nearly the same. However, it is noteworthy that changing the order of the process from direct to reverse mode led to a significant decrease in the standard deviation of the strain values, from 0.408 to 0.111, representing a reduction of 73%. This shift to the reverse extrusion process greatly enhanced the uniformity of the created strains, which is one of the main goals of severe plastic deformation processes.

5.1.3. Hardness

The numerical values of hardness measured at various points across the cross-section of the specimens are presented in Table 6. Hardness values were measured at various radial distances from the center to the perimeter of each specimen.

It is clear that the hardness values in both cases exhibit an increasing trend from the center of the specimen's surface toward the surrounding area. The maximum hardness value is observed in the surrounding area of the specimen.

The measurement results indicate that the average hardness in the reverse extrusion process increased by 9% compared to direct extrusion, however, this change is not considered statistically significant. Given the slight variation in strain, no additional changes in hardness were expected. Furthermore, the standard deviation of hardness distribution in reverse extrusion was 1.9, reflecting a notable decrease of 56% compared to direct extrusion. This substantial improvement demonstrates that reverse extrusion achieves a much more uniform distribution and a more homogeneous structure, which is one of the main goals of all severe plastic deformation processes.

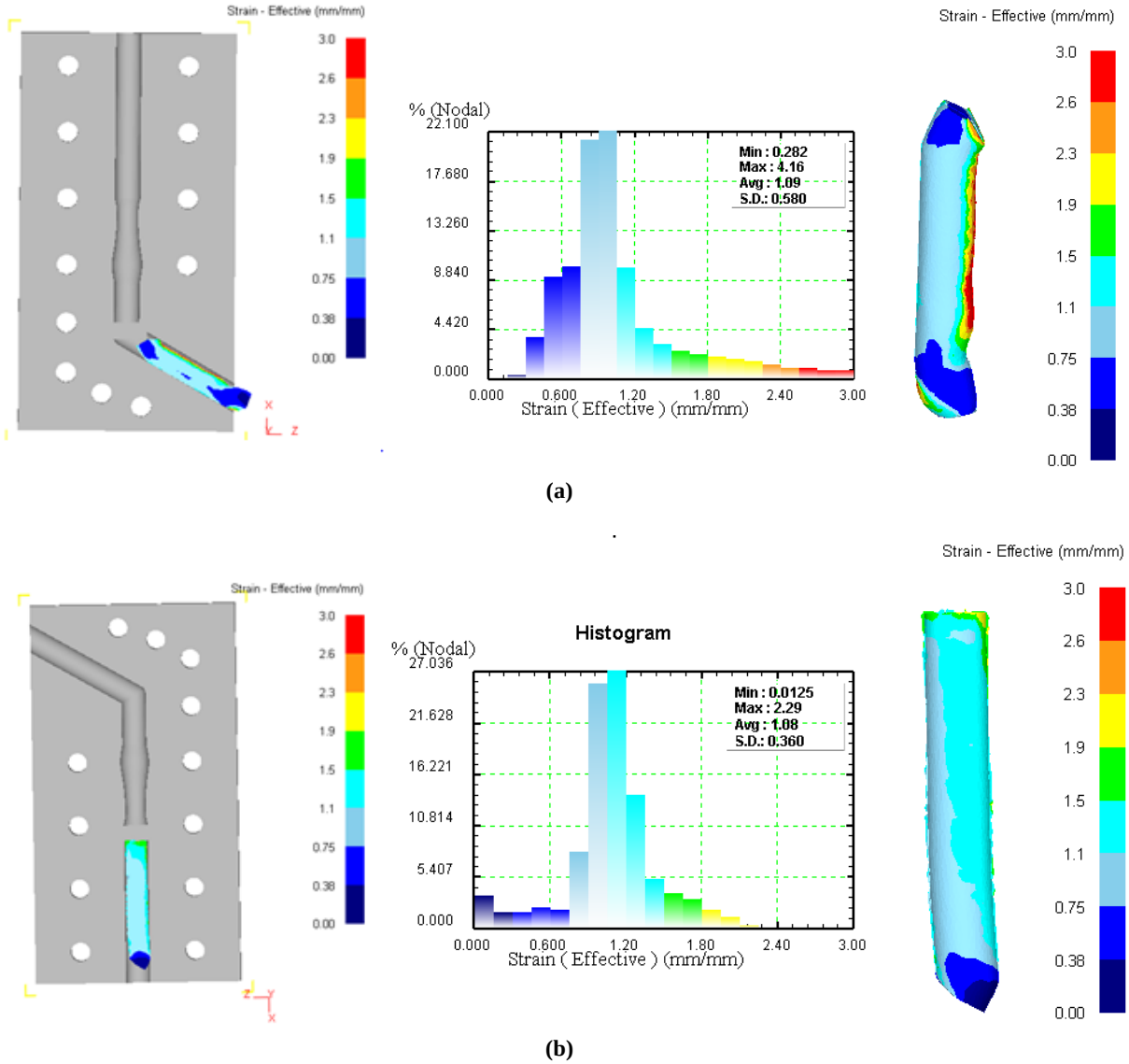

Fig. 12. The strain distribution in the specimen with the histogram diagram of the (a) direct extrusion process and (b) reverse extrusion process.

Table 6. Hardness values measured at at various points across the cross-section of the specimens (Vickers)

Process	Center of the specimen surface	R3 mm	R4 mm	R5 mm	R6 mm	Around specimen	Average hardness	S.D
Annealed specimen	41.1	42.2	43.1	44.9	47	48.2	44.4	2.8
Direct extrusion	116.8	121.9	124.3	125.9	127.1	130.4	124.4	4.3
Reverse extrusion	132.9	134.7	135.8	136.7	137.7	138.3	136	1.9

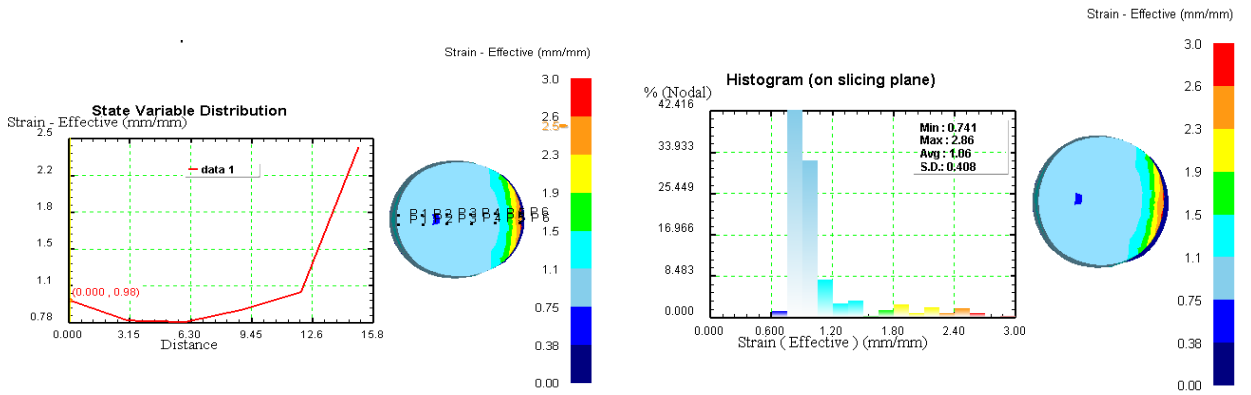

(a)

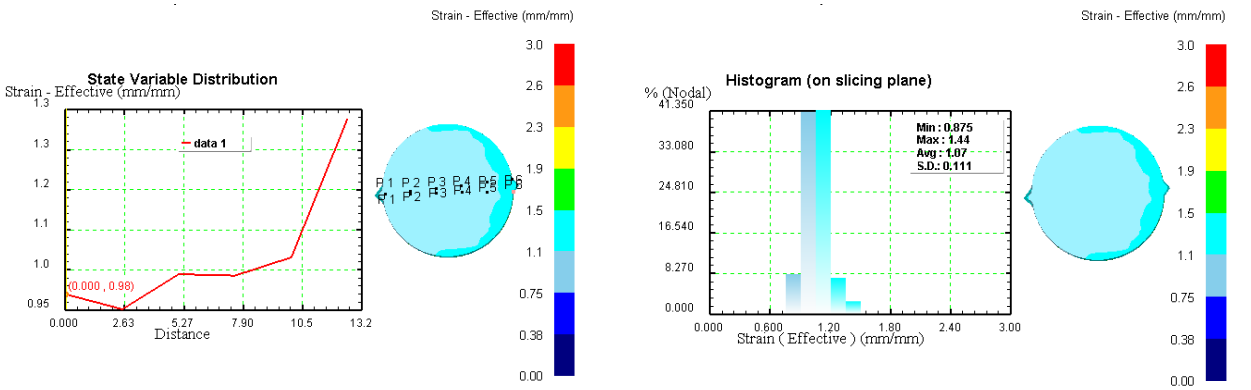

(b)

Fig. 13. Strain distribution curve in the cross-section of the specimen with the histogram diagram of the (a) direct extrusion process, (b) reverse extrusion process.

5.2. Size effect of design variables

5.2.1. Forming force

Fig. 14 illustrates the effect of changes in design variables on the forming force magnitude in seven separate dies.

As can be seen, increasing the value of m from 1.45 in die 6 to values of 1.55 in die 7 and 1.65 in die 5, leads to a transition of the specimen's cross-section from a circular shape to an elliptical one. This transition requires a higher forming force, resulting in an increase in the average forming force, especially in the twisting area. The average forming force in die 6 is at a minimum of 3.26 tons, while in die 5, it rises to 4.82 tons, representing an increase of 48%.

Additionally, increasing the torsion angle θ from 60 degrees in die 4 to 90 degrees in die 3 and 120 degrees in die 1 significantly increases the average forming force, particularly in the torsion area. This increase is attributed to the creation of greater torsional stress in the specimen. The average forming force in die 4 is at a minimum of 2.52 tons, while in die 1, it rises to 3.41 tons, representing an increase of 35%.

Increasing the internal angle of ECAP, α from 90 degrees in die 7 to 105 degrees in die 2 and 120 degrees in die 3 resulted in a decrease in the average forming force, particularly in the ECAP area. This reduction is attributed to the ease of forming the specimen and the corresponding decrease in shear stress within the forming area. The average forming force in die 7 reaches its maximum value of 4.09 tons, while in die 3, this value decreases to 2.76 tons, reflecting a reduction of 33%.

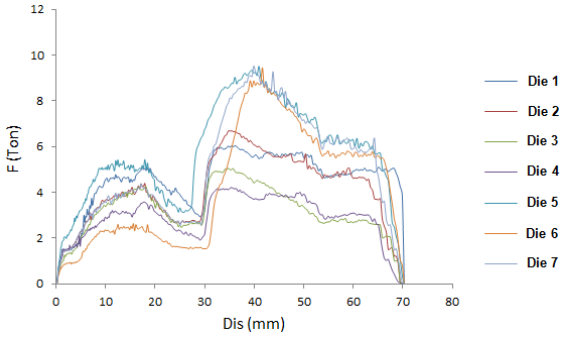

Fig. 14. Comparison of load-displacement diagrams in dies.

5.2.2. Strain

Fig. 15 illustrates the effect of changes in design variables on the created strain in the cross-section of the specimens in 7 dies, separately.

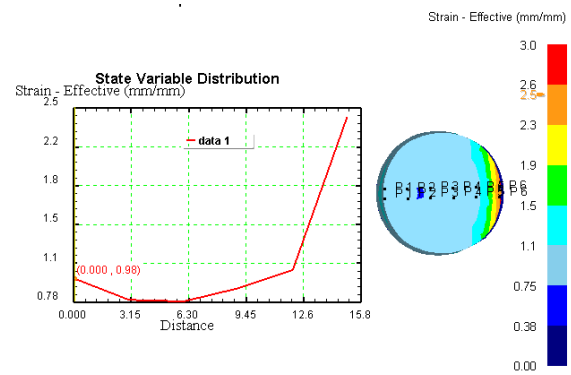

(a)

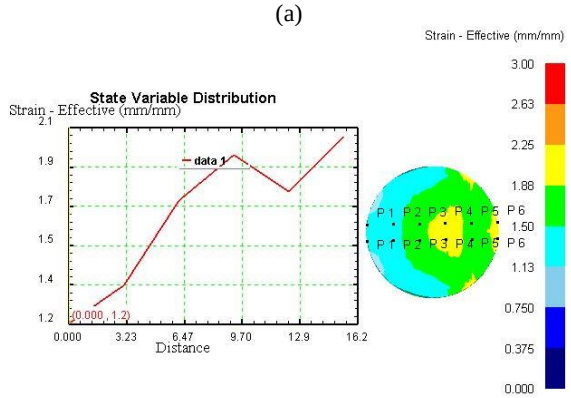

(b)

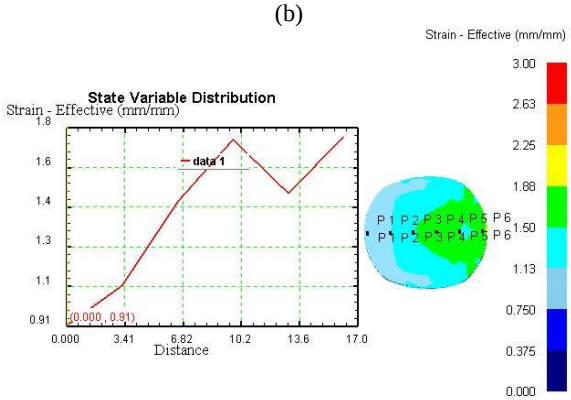

(c)

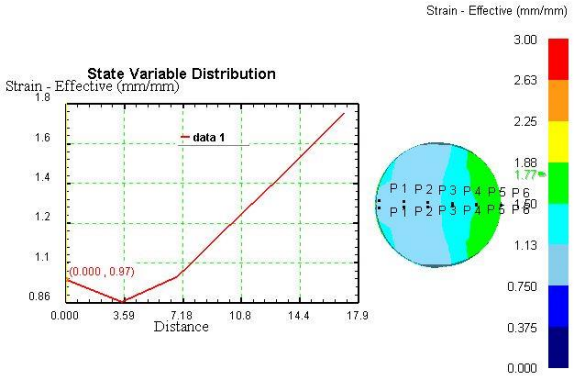

(d)

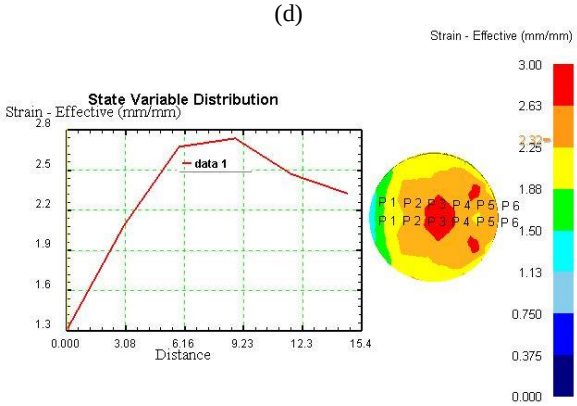

(e)

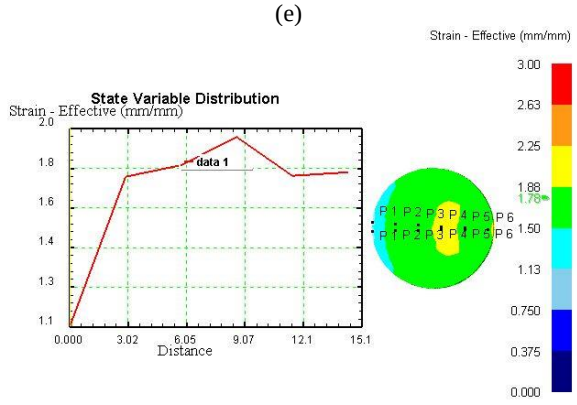

(f)

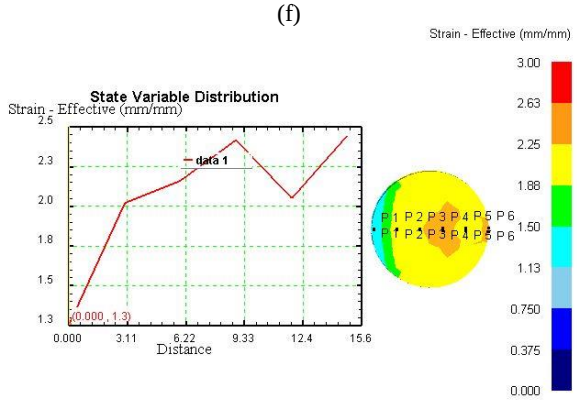

(g)

Fig. 15. Effective strain distribution curve in the cross section of the specimen along with the histogram diagram in the dies: (a) die 1, (b) die 2, (c) die 3, (d) die 4, (e) die 5, (f) die 6, and (g) die 7.

The findings indicate that the increase in the value of m from 1.45 in die 6 to 1.55 in die 7 and 1.65 in die 5 resulted in a larger maximum strain created in the specimen. This increase can be attributed to the transition of the specimen's cross-section from circular to elliptical, which engages more of the specimen with the walls of the die and enhances the effect of friction. The minimum value of strain, which is equal to 1.95, is created in die 6, whereas in die 5, this value rises to 2.8, reflecting a 44% increase. However, the standard deviation of the strains also increased from 0.2 in die 6 to 0.34 in die 5, indicating a decrease in strain uniformity.

Additionally, increasing the twist angle θ from 60 degrees in die 4 to 90 degrees in die 3 and 120 degrees in die 1 cause a rise in the maximum strain created, due to the creation of more torsional stress in the specimen. The maximum strain in die 4 is at a minimum of 1.76, while in die 1, it rises to 2.86, representing an increase of 63%.

Increasing the internal angle of ECAP, α from 90 degrees in die 7 to 105 degrees in die 2 and 120 degrees in die 3 resulted in a decrease in the maximum strain created in the specimen, particularly in the ECAP area. This reduction is attributed to the ease of forming the specimen and the corresponding decrease in shear stress within the forming area. The maximum strain in die 7 reaches its maximum value of 2.46, while in die 3, this value decreases to 1.92, reflecting a reduction of 22%.

6. Conclusion

In the present study, the effect of changing the order of performing the combined process of severe plastic deformation was investigated. The extrusion process of the copper specimen was carried out using a combined die in both direct and reverse modes, and the values of the forming force, strain and hardness created in the specimen were compared with each other. In addition the effects of altering design variables on the forming force and strain values were compared, and the findings are as follows:

- The maximum amount of forming force in the reverse extrusion process compared to direct extrusion increased to about 30%.
- The average amount of strain generated in the two processes was nearly identical. However, in reverse extrusion, the maximum strain value and the standard deviation of the strain values decreased by 50% and 73%, respectively. Creating more uniform strains in just one process pass is one of the advantages of the severe plastic deformation method that was achieved in this research.
- The average hardness in reverse extrusion increased by 9%, which is not considered statistically significant. Due to the slight change in strain in this case, further changes in hardness were not expected. However, the standard deviation of the hardness values decreased by 56%, indicating a much more uniform distribution and a more homogeneous structure.
- Increasing the value of m, leads to a transition of the specimen's cross-section from a circular shape to an elliptical one. This transition requires a higher forming force, resulting in an increase in the average forming force, especially in the twisting area. The minimum value of this parameter was recorded in die 6, while an increase of 48% was observed in die 5.
- As the torsion angle θ increases, more torsional stress is created in the specimen, leading to an increase in the average forming force, particularly in the torsional area. This parameter had its minimum value in die 4 while increasing by 35% in die 1.
- As the internal angle of ECAP, α increases, the reduction in shear stress in the forming area facilitates the process, leading to a decrease in the average forming force. This parameter reached its maximum value in die 7 and decreased by 33% in die 3.
- The increase in the value of m results in a transition of the specimen's cross-sectional area from a circular to an elliptical shape. This transition leads to greater contact between the specimen and the die walls, which, in turn, enhances the effect of friction. As a result, the maximum strain generated in the specimen also increases. The minimum strain value was recorded in die 6, while a 44% increase was observed in die 5. Additionally, the standard deviations of the strains in die 5 increased by 70%

compared to die 6, indicating a decrease in strain uniformity.

- An increase in the twisting angle θ resulted in a corresponding increase in the maximum strain generated in the specimen. The minimum strain value was observed in die 4, while die 1 exhibited a 63% increase in strain.
- As the internal angle of ECAP α increases, the maximum strain generated in the specimen decreases. The maximum strain value was observed in die 7, while in die 3, it decreased by 22%.

Conflict of Interests

The authors state that they have no conflicts of interest to disclose.

Funding

There is no funding available.

7. References

[1] Huang, Y., & Langdon, T. G. (2013). Advances in ultrafine-grained materials. *Materials Today*, *16*(3), 85-93. https://doi.org/10.1016/j.mattod.2013.03.004

[2] Pande, C. S., & Cooper, K. P. (2009). Nanomechanics of Hall–Petch relationship in nanocrystalline materials. *Progress in Materials Science*, *54*(6), 689-706. https://doi.org/10.1016/j.pmatsci.2009.03.008

[3] Roven, H. J. (2007, November 3-9). Nanostructured metals by SPD-technology and commercialization. In *The Second Chinese-Norwegian Symposium on Light Metals*, Shanghai, China.

[4] Rosochowski, A. (2004). Processing metals by severe plastic deformation. *Solid State Phenomena*, *101*, 13-22. https://doi.org/10.4028/www.scientific.net/SSP.101-102.13

[5] Zhu, C. F., Du, F. P., Jiao, Q. Y., Wang, X. M., Chen, A. Y., Liu, F., & Pan, D. (2013). Microstructure and strength of pure Cu with large grains processed by equal channel angular pressing. *Materials & Design (1980-2015)*, *52*, 23-29. https://doi.org/10.1016/j.matdes.2013.05.029

[6] Xue, K., Luo, Z., Xia, S., Dong, J., & Li, P. (2024). Study of microstructural evolution, mechanical properties and plastic deformation behavior of Mg-Gd-Y-Zn-Zr alloy prepared by high-pressure torsion. *Materials Science and Engineering: A*, *891*, 145953. https://doi.org/10.1016/j.msea.2023.145953

[7] Samadzadeh, M., Toroghinejad, M. R., Mehr, V. Y., Asgari, H., & Szpunar, J. A. (2024). Mechanical, microstructural, and textural evaluation of aluminum-MWCNT composites manufactured via accumulative roll bonding at ambient condition. *Materials Chemistry and Physics*, *315*, 128891. https://doi.org/10.1016/j.matchemphys.2024.128891

[8] Noor, S. V., Eivani, A. R., Jafarian, H. R., & Mirzaei, M. (2016). Inhomogeneity in microstructure and mechanical properties during twist extrusion. *Materials Science and Engineering: A*, *652*, 186-191. https://doi.org/10.1016/j.msea.2015.11.056

[9] Naik, M. V., Narasaiah, N., Chakravarthy, P., & Kumar, R. A. (2024). Microstructure and mechanical properties of friction stir processed Zn-Mg biodegradable alloys. *Journal of Alloys and Compounds*, *970*, 172160. https://doi.org/10.1016/j.jallcom.2023.172160

[10] Wang, C., Li, F., Li, Q., Li, J., Wang, L., & Dong, J. (2013). A novel severe plastic deformation method for fabricating ultrafine grained pure copper. *Materials & Design*, *43*, 492-498. https://doi.org/10.1016/j.matdes.2012.07.047

[11] Djavanroodi, F., Ebrahimi, M., Rajabifar, B., & Akramizadeh, S. (2010). Fatigue design factors for ECAPed materials. *Materials Science and Engineering: A*, *528*(2), 745-750. https://doi.org/10.1016/j.msea.2010.09.080

[12] Kang, D. H., & Kim, T. W. (2010). Mechanical behavior and microstructural evolution of commercially pure titanium in enhanced multi-pass equal channel angular pressing and cold extrusion. *Materials & Design*, *31*, S54-S60. https://doi.org/10.1016/j.matdes.2010.01.004

[13] Nakashima, K., Horita, Z., Nemoto, M., & Langdon, T. G. (2000). Development of a multi-pass facility for equal-channel angular pressing to high total strains. *Materials Science and Engineering: A*, *281*(1-2), 82-87 https://doi.org/10.1016/s0921-5093(99)00744-3

[14] Latypov, M. I., Alexandrov, I. V., Beygelzimer, Y. E., Lee, S., & Kim, H. S. (2012). Finite element analysis of plastic deformation in twist extrusion. *Computational Materials Science*, *60*, 194-200. https://doi.org/10.1016/j.commatsci.2012.03.035

[15] Jiang, J. F., Ying, W. A. N. G., Liu, Y. Z., Xiao, G. F., & Hua, L. I. (2021). Microstructure and mechanical properties of 7005 aluminum alloy processed by one-pass equal channel reciprocating extrusion. *Transactions of Nonferrous Metals Society of China*, *31*(3), 609-625. https://doi.org/10.1016/S1003-6326(21)65523-1

[16] Gupta, B., Kapoor, A., Singhal, A., & Agarwal, K. M. (2021, July). Effect of die design parameters on materials processed by equal channel angular pressing. In *IOP Conference Series: Materials Science and Engineering* (Vol. 1168, No. 1, p. 012005). IOP Publishing. https://doi.org/10.1088/1757-899X/1168/1/012005

[17] Muralidharan, S., & Iqbal, U. M. (2022). Experimental studies and optimization of process variables in multi-angular twist extrusion (MATE) of Cu-Cr-Zr alloy. *Materials Today: Proceedings*, *68*, 1835-1844. https://doi.org/10.1016/j.matpr.2022.07.411

[18] Attarilar, S., Gode, C., Mashhuriazar, M. H., & Ebrahimi, M. (2021). Tailoring twist extrusion process; the better strain behavior at the lower required loads. *Journal of Alloys and Compounds*, *859*, 157855. https://doi.org/10.1016/j.jallcom.2020.157855

[19] Zamani, S. A., Bakhshi-Jooybari, M., Gorji, H., Hosseinipour, S. J., & Hoseinzadeh-Amirdehi, M. (2021). Investigation of the effect of die parameters on the mechanical properties of pure copper in The combined process of torsional extrusion and ECAP. *Journal of Stress Analysis*, *5*(2), 83-99. https://doi.org/10.22084/jrstan.2021.23800.1174

[20] Kočiško, R., Kvačkaj, T., & Kováčová, A. (2014). The influence of ECAP geometry on the effective strain distribution. *Journal of Achievements in Materials and Manufacturing Engineering*, *62*, 25-30. https://doi.org/10.4028/www.scientific.net/AMR.1127.135

[21] Bisadi, H., Mohamadi, M. R., Miyanaji, H., & Abdoli, M. (2013). A modification on ECAP process by incorporating twist channel. *Journal of Materials Engineering and Performance*, *22*, 875-881. https://doi.org/10.1007/s11665-012-0323-z

[22] Wang, C., Li, F., Li, Q., Li, J., Wang, L., & Dong, J. (2013). A novel severe plastic deformation method for fabricating ultrafine grained pure copper. *Materials & Design*, *43*, 492-498. https://doi.org/10.1016/j.matdes.2012.07.047

[23] Wang, C., Li, F., Lu, H., Yuan, Z., & Chen, B. (2013). Optimization of structural parameters for elliptical cross-section spiral equal-channel extrusion dies based on grey theory. *Chinese Journal of Aeronautics*, *26*(1), 209-216. https://doi.org/10.1016%2Fj.cja.2012.12.012

[24] Heydari Pebdani, F., Nourbakhsh, S. H., & Akbaripanah, F. (2022). Effects of the geometric profile of twist channel angular pressing (TCAP) on the deformation behaviors and microstructure evolution of AL7050 alloy. *Journal of Stress Analysis*, *6*(2), 85-95. https://doi.org/10.22084/jrstan.2022.26081.1207

[25] Hosseinzadeh, M., & Mouziraji, M. G. (2016). An analysis of tube drawing process used to produce squared sections from round tubes through FE simulation and response surface methodology. *The International Journal of Advanced Manufacturing Technology*, *87*(5), 2179-2194. https://doi.org/10.1007/s00170-016-8532-5

[26] Djavanroodi, F., Zolfaghari, A. A., Ebrahimi, M., & Nikbin, K. M. (2013). Equal channel angular pressing of tubular samples. *Acta Metallurgica Sinica (English Letters)*, *26*, 574-580. https://doi.org/10.1007/s40195-013-0102-3